

# Topological characterization of crystalline ice structures from coordination sequences

Carlos P. Herrero and Rafael Ramírez

*Instituto de Ciencia de Materiales de Madrid, Consejo Superior de Investigaciones Científicas (CSIC), Campus de Cantoblanco, 28049 Madrid, Spain*

(Dated: September 10, 2018)

Topological properties of crystalline ice structures are studied by considering ring statistics, coordination sequences, and topological density of different ice phases. The coordination sequences (number of sites at topological distance  $k$  from a reference site) have been obtained by direct enumeration until at least 40 coordination spheres for different ice polymorphs. This allows us to study the asymptotic behavior of the mean number of sites in the  $k$ -th shell,  $M_k$ , for high values of  $k$ :  $M_k \sim ak^2$ ,  $a$  being a structure-dependent parameter. Small departures from a strict parabolic dependence have been studied by considering first and second differences of the series  $\{M_k\}$  for each structure. The parameter  $a$  ranges from 2.00 for ice VI to 4.27 for ice XII, and is used to define a topological density for these solid phases of water. Correlations between such topological density and the actual volume of ice phases are discussed. Ices Ih and Ic are found to depart from the general trend in this correlation due to the large void space in their structures.

## I. INTRODUCTION

Water presents a large variety of solid structures, and up to now sixteen different crystalline ice phases have been found.<sup>1-4</sup> A large amount of experimental and theoretical work has been devoted to determine precisely their crystal structures and stability range in the pressure-temperature phase diagram. Notwithstanding the broad knowledge so obtained, some properties of these solid phases still lack a full understanding. This is mainly owing to the presence of hydrogen bonds between contiguous molecules, which gives rise to some peculiarities in their properties (the so-called ‘water anomalies’).<sup>5-7</sup>

Water molecules appear in all known ice phases (with the exception of ice X) as well defined entities building up a network linked by H-bonds. In such a network each water molecule is bound to four others in a more or less distorted tetrahedral coordination. The orientation of each molecule with respect to its four nearest neighbors complies with the so-called Bernal-Fowler ice rules. These rules state that each H<sub>2</sub>O molecule is oriented so that its two hydrogen atoms point toward contiguous oxygen atoms and there is exactly one hydrogen between two adjacent oxygen atoms.<sup>8</sup>

Oriental disorder of the water molecules appears in several ice phases. Though oxygen atoms display full occupancy ( $f$ ) of their crystallographic sites, hydrogen atoms may present a disordered distribution, as shown by a fractional occupancy of their lattice positions. Thus, hexagonal ice Ih, the stable phase of solid water under normal conditions, presents full hydrogen disorder compatible with the ice rules (occupancy of H-sites  $f = 0.5$ ). However, some phases such as ice II are H-ordered, whilst others as ices III and V are characterized by partial hydrogen order (some fractional occupancies  $f \neq 0.5$ ).

Given the variety of ice structures, some unifying classification can help to deeper understanding of their physical and chemical properties.<sup>3,9</sup> Most classification schemes of crystalline solids are based on the space symmetry and/or the short-distance atomic environments.

In other schemes, attention is focused on geometrical aspects of packing of structural units. Such classification methods can be considered as geometrical, as their main criteria are geometrical properties of crystal structures.<sup>10-13</sup> A difficult issue of these geometrical classification methods can be the involvement of finding relations between compounds whose structures are distorted. Another possibility is the use of classification schemes based on topological criteria, i.e., putting emphasis on the organization of the interatomic bonds in a crystal structure as a basic criterion for a crystal-chemical analysis. Thus, topological properties of crystal structures have been taken into account in the past to describe different kinds of materials.<sup>10-12</sup>

A discussion of the network topologies of different ice polymorphs and the relation of ring sizes in the various phases with the crystal volume has been presented by Salzmann *et al.*<sup>3</sup> Topological studies of three-dimensional hydrogen-bonded frameworks in organic crystals have also helped to classify this kind of structures.<sup>14</sup> Moreover, the topology of hydrogen-bond networks in ice has been considered in order to analyze hydrogen ordering. In particular, graph invariants have turned out to be very useful to obtain the energy of hydrogen configurations on a given ice network.<sup>15-17</sup> Graph theory has been also used to study isotypism in crystal structures.<sup>13</sup>

To characterize the ice structures from a topological point of view, we will employ the so-called coordination sequences. This is a generalization of the coordination number, usually known as the number of nearest neighbors of an atom in a solid structure. In this respect, an ice structure can be viewed as a three-dimensional hydrogen-bonded network, and thus one can consider a simplified structure where each oxygen atom is assumed to be linked to four other oxygen atoms, without explicit mention of the hydrogen atoms lying between them. Then, for a particular site, one defines a coordination sequence as a series of numbers  $\{N_k\}$  ( $k = 1, 2, \dots$ ), where  $N_k$  is the number of sites located at a topological distance  $k$  from the reference (see below). Note that this

is a purely topological concept, as the coordination sequence for each oxygen atom in an ice structure depends only on the topology of the network, but not on lattice distortions and other structural factors.

The concept of coordination sequence was applied to silicate frameworks by Meier and Moeck in 1979.<sup>18</sup> Since then, several authors employed this concept to characterize from a topological point of view different types of materials<sup>19–24</sup> and complex networks.<sup>25</sup> Coordination sequences can be used to define a topological density, as a structural characteristic related to the increase in the number  $N_k$  of sites accessible through  $k$  links in a given structure. In this paper, we analyze this question by calculating the coordination sequence for crystalline phases of ice, up to at least  $k = 40$ , and thus approaching the asymptotic behavior of  $\{N_k\}$  at large distances. A definition of topological density can be derived from such an asymptotic behavior.

This kind of topological studies are relevant to connect the small-scale characteristics of solid water to macroscopic features such as mechanical or plastic properties, not only for crystalline structures but also for various types of amorphous ice, as well as liquid water.<sup>6</sup> Moreover, networks of water molecules are paradigmatic in the study of compounds for which H-bonds play a significant role in their structural, dynamical, and electronic properties.

## II. COMPUTATIONAL METHOD

Our model is defined in the following way. We consider an ice structure as defined by the positions of the oxygen atoms, so that each O atom has four nearest neighbors. This defines a network, where the nodes are the O sites, and the links are H-bonds between nearest neighbors. The network coordination is four, which gives a total of  $2N$  links,  $N$  being the number of nodes. We implicitly assume that on each link there is one H atom, but its consideration is not relevant for our present purposes.

For a given network, we define the ‘topological distance’ between two sites as the number of bonds in the shortest path connecting one site to the other. This is obviously a symmetric property, in the sense that the topological distance from site A to site B is the same as that from B to A. We will call  $N_k$  the number of sites at a topological distance  $k$  from a given node, i.e. in its  $k$ ’th ‘coordination shell’. This is a generalization of the usual coordination shell formed by nearest neighbors in solid structures ( $k = 1$ ). Then, we call the sequence  $\{N_k\}$  the ‘coordination sequence’ of this node. In general, different nodes in a network may have different coordination sequences, and we will call coordination sequence of a network to the sequence  $\{M_k\}$ , where each  $M_k$  is obtained by averaging the  $N_k$  values for the oxygen sites in the unit cell. For ice structures including O sites topologically non-equivalent (e.g., ices III, IV, V, VI, and XII), relative differences between  $N_k$  values corresponding to

sites in a given structure decrease fast with the distance  $k$ . In fact, the relative difference is about 0.1% for  $k = 40$ , and becomes negligible in the large- $k$  limit.

TABLE I: Crystal system and space group for the ice polymorphs considered in this work.

Phase	Crystal system	Space group	Ref.
Ih	Hexagonal	$P6_3/mmc$ , 194	64
Ic	Cubic	$Fd\bar{3}m$ , 227	65
II	Rhombohedral	$R\bar{3}$ , 148	66
III	Tetragonal	$P4_12_12$ , 92	67
IV	Rhombohedral	$R\bar{3}c$ , 167	68
V	Monoclinic	$A2/a$ , 15	67
VI	Tetragonal	$P4_2/nmc$ , 137	69
XII	Tetragonal	$I\bar{4}2d$ , 122	70

For some solid structures, it is known that one can find regularities in the sequence  $\{M_k\}$  for relatively low values of the topological distance  $k$ ,<sup>21</sup> and thus easily extrapolate to the behavior of  $\{M_k\}$  at large distances. In general, however, a study of the asymptotic behavior of coordination sequences for a given network requires the generation of large supercells. For the ice structures considered in this work, supercells including around  $3 \times 10^5$  oxygen sites were generated from structural data taken from the literature. The relevant information on these structural data is presented in Table I. Then, given an oxygen site, numbers of sites  $N_k$  in successive coordination shells were obtained by direct enumeration. To this end, one only needs to assign a label (e.g., a number) to each node in the considered supercell, and associate it with those corresponding to its four nearest neighbors. Thus, given a node, one finds successively its first neighbors, then the neighbors of these, and so on, with the precaution of not going ‘backwards’, i.e., not counting again sites already visited in a previous step.

It is important to realize that the coordination sequence for each site in a given structure depends only on the topology of the network, and not on the actual symmetry, cell parameters, or other structural data. In particular, the coordination sequence  $\{M_k\}$  for a given ice structure is not affected by the ordering of H atoms. This means that structures such as those of ices Ih and XI (the former being H-disordered and the latter H-ordered), with the same topology, will have the same sequence  $\{M_k\}$ . There are five other pairs of ice structures sharing the same topology, and connected one with the other through an order/disorder phase transition. Thus, one has six pairs of ice structures: Ih-XI, III-IX, V-XIII, VI-XV, VII-VIII, and XII-XIV.<sup>3</sup> In each pair, the first structure is H-disordered, and the second is H-ordered. In the following, for our topological characterization we will only refer to the disordered case, but meaning that it represents both members of the corresponding pair.

Apart from these, there are ice structures with topology different from that of the structures above, and for which no pair has been found: ice Ic (H-disordered), ice II (H-ordered), and ice IV (H-disordered). There is also the structure of ice X, which is topologically equivalent to those of ices VII and VIII, but with the main difference that in ice X hydrogen atoms lie at the middle point between oxygen atoms, and water molecules lose in fact their own entity (this is however irrelevant for our topological characterization). Then, we have 9 topologically different ice structures. We note that the network associated to ice VII (as well as ices VIII and X) is made up of two interpenetrating but disjoint subnetworks, each of them equivalent to the ice Ic network, and therefore with its same topology. There is another case, the pair VI-XV, for which the network consists of two independent subnetworks, but they are not equivalent to the network of any other known ice structure. For these reasons we will consider the 8 structures listed in Table I, where we indicate the crystal system, space group, and the reference we used to generate the corresponding supercells.

Coordination sequences corresponding to structures in  $D$ -dimensional space increase with topological distance  $k$  roughly as  $k^{D-1}$ .<sup>19,20</sup> Then, for three-dimensional structures one expects for large  $k$  a dependence

$$M_k \sim a k^2 \quad , \quad (1)$$

where  $a$  is a network-dependent parameter. Thus,  $M_k$  increases quadratically with  $k$  just as the surface of a sphere increases quadratically with its radius. This is in fact the dependence found for different kinds of real materials.<sup>21,23</sup> In general, including also small values of  $k$ , a quadratic dependence of the form

$$M_k = a k^2 + b k + c \quad (2)$$

has been found to follow closely the coordination sequences of actual structures.<sup>21,23</sup> Given a dependence such as Eq. (2), the parameters  $b$  and  $c$  become irrelevant for large distances, and one has  $M_k/k^2 \rightarrow a$ . Such a parabolic dependence, although it follows closely the sequence  $\{M_k\}$  for solid structures, is not strictly followed in general. Thus, it is well known for the diamond structure (ice Ic in our case) that the equation  $M_k = 2.5 k^2 + 1.75$  yields values too high by 0.25 if  $k$  is odd and too low by 0.25 if  $k$  is even.<sup>19,21</sup>

To characterize the coordination sequences of ice structures, and in particular their deviation from strict parabolic behavior, we will consider first and second differences. We define the first differences of a sequence  $\{M_k\}$  as

$$\delta_k = M_{k+1} - M_k \quad (3)$$

and the second differences as

$$\epsilon_k = \frac{1}{2}(\delta_k - \delta_{k-1}) = \frac{1}{2}(M_{k+1} - 2M_k + M_{k-1}) \quad (4)$$

Note the factor 1/2 in Eq. (4), introduced for the sake of comparison with the parameter  $a$  in Eq. (2). In fact, for

a strict parabolic dependence of  $M_k$  on  $k$ , as in Eq. (2), one would have a constant second difference  $\epsilon_k = a$  for all  $k$ .

Since the parameter  $a$  is a quantitative measure of the mean number of sites connected to a given site in a finite number of steps on the corresponding network, we define the ‘topological density’  $\rho$  as

$$\rho = w a \quad , \quad (5)$$

where  $w$  is the number of disconnected subnetworks in the considered network. Usually  $w = 1$ , but for the ice structures including two interpenetrating networks (as ices VI and VII) one has  $w = 2$ .

For a given network, we call  $S_k$  the mean number of sites up to coordination shell  $k$ , without counting the starting site (this has been called in the literature<sup>20</sup> a ‘crystal ball’ of radius  $k$ ):

$$S_k = \sum_{i=1}^k M_i \quad (6)$$

This quantity has been employed earlier to quantify the topological density of crystal structures.<sup>26</sup>

To investigate the relation between topological density and real density of ice structures, we will compare values of  $\rho$  with those of the volume per molecule  $v$ . In this respect, it is important to remember that the different ice structures are stable in some cases at very different conditions of pressure and temperature. This means that a direct comparison of  $v$  values for different phases with their corresponding topological densities may be misleading, as  $\rho$  is independent of bond lengths, lattice distortions, and other structural characteristics that may dramatically change with pressure and/or temperature.

To avoid this problem, we will consider for each ice structure a reference volume  $v_0$ , defined as the volume per molecule that minimizes the potential energy of the crystal at zero pressure. For this purpose we need a reliable potential model. We have used the point charge, flexible q-TIP4P/F model, developed to study liquid water,<sup>27</sup> and that has been used later to study various properties of ice<sup>28,29</sup> and water clusters.<sup>30</sup> This interatomic potential takes into account the significant anharmonicity of the O–H vibration in a water molecule by considering anharmonic stretches. The q-TIP4P/F interaction model has turned out to give reliable results for several ice phases, and in particular it predicts crystal volumes in fairly good agreement with experimental data.<sup>29,31</sup> For each ice structure, determination of the reference volume was carried out by an energy minimization, where both atomic positions and cell parameters were optimized. Details on this minimization procedure can be found elsewhere.<sup>31</sup>

TABLE II: Number and size ( $L$ ) of the rings appearing in different ice structures.  $m_j$  is the label of the crystallographic position of the oxygen atoms. The numeral in the label indicates the multiplicity of the site in the considered unit cell. For ices II and IV the given crystallographic positions correspond to the choice of a rhombohedral cell in the space group.  $x(L)$  indicates the fraction of loops in an ice structure for each size  $L$ .  $\langle L \rangle$  is the mean loop size, as defined in Eq. (9).

Ice	Site $j$	$m_j$	$L$								$\langle L \rangle$
			4	5	6	7	8	9	10	12	
Ih	1	4f	-	-	12	-	-	-	-	-	
	2	4f	-	-	12	-	-	-	-	-	
	$x(L)$				1.0						6
Ic	1	8a	-	-	12	-	-	-	-	-	
	$x(L)$				1.0						6
	II	1	6f	-	-	7	-	12	-	25	-
	2	6f	-	-	7	-	12	-	25	-	
	$x(L)$				0.226		0.290		0.484		8.52
III	1	4a	-	4	-	4	4	-	-	-	
	2	8b	-	3	-	5	6	-	-	-	
	$x(L)$			0.333		0.333	0.333				6.67
IV	1	4c	-	-	6	-	12	-	63	-	
	2	12f	-	-	5	-	20	-	49	-	
	$x(L)$				0.104		0.269		0.627		9.04
V	1	4e	-	3	2	-	2	4	24	2	
	2	8f	1	3	2	-	3	2	16	1	
	3	8f	1	1	2	-	4	3	18	2	
	4	8f	2	2	1	-	4	2	14	2	
	$x(L)$		0.08	0.12	0.08		0.12	0.08	0.48	0.04	8.36
VI	1	2a	4	-	-	-	16	-	-	-	
	2	8g	4	-	-	-	14	-	-	-	
	$x(L)$		0.357				0.643				6.57
XII	1	4a	-	-	-	8	16	-	-	-	
	2	8d	-	-	-	10	16	-	-	-	
	$x(L)$					0.4	0.6				7.6

### III. RESULTS AND DISCUSSION

#### A. Rings

Given the variety of known crystalline ice structures, it is not strange that the coordination of water molecules further than nearest neighbors may display clear differences between different structures, as could be expected from the pressure/temperature range where they are stable. In this line, as a first characteristic observable in the ice networks, we consider rings of water molecules, which define the particular topology of each structure. A discussion of the structural variation in tetrahedral networks was presented by Zachariasen as early as 1932,<sup>32</sup> and a

systematic description of the topology of different network types was given by Bernal,<sup>33</sup> who suggested that rings should be a basic topological measure, in particular for covalently bonded structures.<sup>34-36</sup>

In general, a ring may be defined as any returning path in a network. This definition is however not very useful, as there is an infinite number of those rings. For practical reasons, it is desirable to identify a small set of rings as fundamental topological units. Following Mariani and Hobbs,<sup>37</sup> we will define a fundamental ring as any ring that cannot be divided into two smaller ones. Thus, in the computer code employed to analyze the ice structures, we first find loops in a given network, and then we check for each one that there is no possible ‘shortcut’

between any pair of sites in the loop, as this would mean that the loop could be divided into two smaller ones. This definition coincides with that employed by Salzmann *et al.*<sup>3</sup> to analyze correlations between ring size and density of ice polymorphs. Note that we call simply rings (or structural rings) what has been called ‘minimal rings’ by Guttman,<sup>36</sup> ‘strong rings’ by Goetzke and Klein,<sup>38</sup> or ‘primitive rings’ by Yuan and Cormack<sup>39</sup> in their studies of different types of materials and topological networks. Other definitions, non-equivalent to that given here, have been presented in the literature. In particular, for Goetzke and Klein,<sup>38</sup> a loop is a ‘very strong ring’ if it contains some link which is not a member of some shorter ring. This set of rings is a subset of those considered here, and is interesting in graph theory for its properties as a covering set, i.e., the set of very strong rings of a graph is always a cover of all links of cycles of the graph. This property and ring definitions related to it are of no particular interest for our present purposes, and thus our definition is taken to be consistent with those mentioned above and employed earlier to characterize several types of materials, including ice polymorphs.<sup>3</sup>

Calling  $n_j(L)$  the number of rings of size  $L$  which include a given site of type  $j$ , the number of  $L$ -membered rings per unit cell is

$$r(L) = \sum_j m_j \frac{n_j(L)}{L} \quad (7)$$

where  $m_j$  is the multiplicity of site  $j$  in the unit cell. Then, the fraction  $x(L)$  of rings of size  $L$  is

$$x(L) = \frac{r(L)}{R}, \quad R = \sum_L r(L) \quad (8)$$

and the mean ring size  $\langle L \rangle$  is given by

$$\langle L \rangle = \sum_L L x(L) \quad (9)$$

For each structure and ring size, we present in Table II the number of rings which include a given network site. We give separately results for the different crystallographic sites in each structure, as they may have different topological environment. It is clear that crystallographically equivalent sites are topologically equivalent, and therefore have the same coordination sequence, but sites crystallographically non-equivalent may be topologically equivalent or not. In several ice structures all sites are topologically equivalent (homogeneous networks<sup>18</sup>), as we observe for ices Ih, Ic, and II, where the number and size of the rings coincide for all sites in each structure. In other structures, however, there appear several (up to 4) topologically distinct sites (heterogeneous networks<sup>18</sup>), and different crystallographic sites have different topological environments (see Table II).

A distinct property of ices Ih and Ic is that all rings in their crystal structures have the same size (six-membered

rings,  $L = 6$ ). Ices VI and XII display rings of two different sizes ( $L = 4$  and 8 for ice VI; 7 and 8 for ice XII). The largest variety of ring sizes corresponds to ice V, for which one finds rings of seven different sizes. The minimum ring size found in the considered structures is four, which appears for ices V and VI. The largest loops contain 12 sites, and only appear in ice V. In Table II we also present the mean ring size  $\langle L \rangle$  for each ice polymorph. The smallest mean size is six (for ices Ih and Ic), and the largest amounts to 9.04 (for ice IV). Average ring sizes smaller than six have been found in the water networks of various clathrate hydrates.<sup>40</sup>

It is known that the structure of water in confined regions appreciably differs from those of the bulk liquid and solid phases, and one may find peculiar topologies for the hydrogen-bond networks in those cases.<sup>41–44</sup> In particular, for water-filled carbon nanotubes the H-bond network consists of stacked  $L$ -membered rings, where  $L$  goes from 4 to 6 depending on the nanotube diameter.<sup>45,46</sup> Infrared spectroscopy has allowed in this case to detect distinct vibrational frequencies associated to intra- and inter-ring hydrogen bonds,<sup>43</sup> revealing this technique as a reliable complementary tool to diffraction studies in the topological characterization of confined water.<sup>41</sup> Similar procedures can be also used to study the actual topology of various phases of amorphous ice, where experimental techniques and simulations have been shown to yield complementary information on this matter.<sup>46–51</sup>

## B. Coordination sequences

We now turn to the coordination sequences of the different ice structures. In Table III we give the mean values  $M_k$  of the coordination sequence of the considered structures for several values of the topological distance  $k$ . We show in particular the first terms in the sequence (for  $k = 2, 3$ , and 4) to see the effect of structural rings. We present also  $M_k$  for larger  $k$  values, such as  $k = 10, 20$ , and 30. The accumulated number of sites up to  $k = 30$  is given by  $S_{30}$  for each structure. The coordination sequence of ice Ih is the same as that of  $\beta$ -tridymite silica, as both structures have the same topology. Also, the sequence  $\{M_k\}$  for ice Ic coincides with that of  $\beta$ -cristobalite and diamond.<sup>19</sup>

For a network without loops (Bethe lattice<sup>22,52</sup>), the coordination sequence is given by

$$M_k^B = z(z-1)^{k-1} \quad (10)$$

where  $z$  is the number of nearest neighbors (degree or connectivity in the language of graph theory), assumed to be the same for all sites ( $z = 4$  here). For actual crystal structures, whose networks include loops,  $M_k$  will be in general smaller than  $M_k^B$ . The number of sites at topological distance  $k$ ,  $M_k$ , is affected by the number of structural rings of size  $L \leq k/2$ . For example, the presence of a four-membered ring causes a reduction of one node in the second coordination shell ( $k = 2$ ); five-

TABLE III: Average number of sites  $M_k$  for  $k = 2, 3, 4, 10, 20,$  and  $30$ , for different ice structures, along with the corresponding parameter  $a$  obtained from a fit to the equation  $M_k = ak^2 + bk + c$ .  $S_{30}$  is the total number of sites up to  $k = 30$ .  $\rho/\rho_{\text{Ih}}$  is the relative topological density with respect to ice Ih. On the last column, P and NP indicate whether the sequence  $\{\epsilon_k\}$  was found to be periodic or non-periodic; when a period was found, a number indicates its length.

Ice	$M_2$	$M_3$	$M_4$	$M_{10}$	$M_{20}$	$M_{30}$	$S_{30}$	$a$	$\rho/\rho_{\text{Ih}}$	$\{\epsilon_k\}$
Ih	12	25	44	264	1052	2364	24866	2.62	1	P 4
Ic	12	24	42	252	1002	2252	23690	2.50	0.95	P 2
II	12	29	58	346	1392	3136	32897	3.50	1.34	P 4
III	12	28	49.3	319.3	1289.3	2907.3	30474	3.24	1.24	NP
IV	12	31	65	402	1629.5	3681	38486	4.12	1.57	NP
V	10.9	24.9	53.1	379.4	1530	3464.6	36207.1	3.86	1.47	NP
VI	8.8	18.8	34.4	201.6	802.4	1800.4	18956.8	2.00	1.53	P 12
XII	12	36	62	417.3	1686.7	3814.7	39957.3	4.27	1.63	P 20

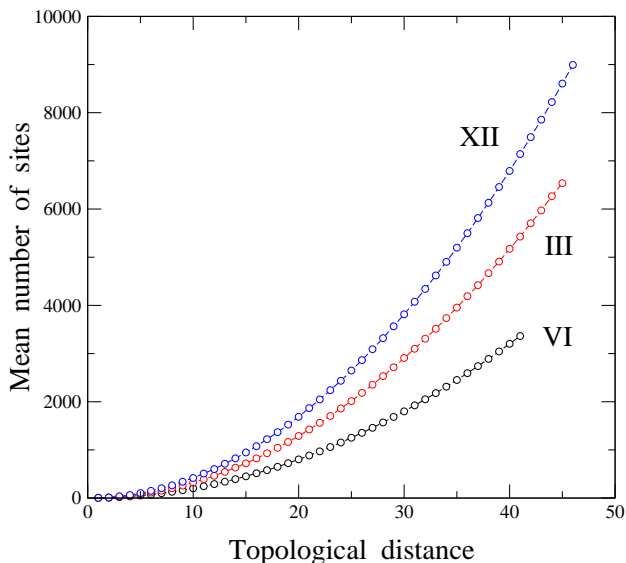


FIG. 1: Coordination sequences  $\{M_k\}$  of three ice structures vs topological distance  $k$ . From top to bottom: ice XII, III, and VI.

and six-membered rings affect the coordination sequence for  $k \geq 3$ , and so on.

The lower terms of the sequence  $\{M_k\}$  are especially indicative of the relative abundance of small rings, as such rings appreciably contribute to decrease the  $M_k$  values. None of the known crystalline ice structures contain 3-membered rings. For structures not including 4-membered rings, one has  $M_2 = 12$  (the maximum value allowed by Eq. (10)). Ices V and VI contain 4-membered rings, and their mean  $M_2$  values are 10.9 and 8.8, respectively. In the same way, 5- and 6-membered rings contribute to decrease  $M_3$  from its possible maximum value ( $M_3^B = 36$ ) for all considered structures, with the exception of ice XII, for which the smallest loops include seven water molecules (see Table II).

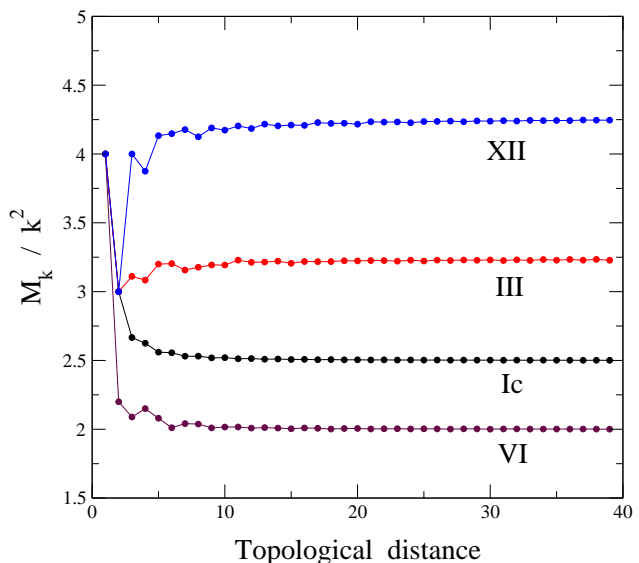


FIG. 2: Ratio  $M_k/k^2$  vs topological distance  $k$  for several ice structures. For large  $k$  this ratio converges to the coefficient  $a$  of the second-order term in Eq. (2). From top to bottom: ice XII, III, Ic, and VI.

In Fig. 1 we show the coordination sequence  $\{M_k\}$  for three ice structures (ices III, VI, and XII) up to  $k \sim 40$ . One observes the apparent parabolic dependence for  $\{M_k\}$  in all cases, but with clearly different slopes. Thus, for ice XII,  $M_{40}$  is more than twice the corresponding value for ice VI, in agreement with the difference obtained for the coefficient  $a$  of  $k^2$  in Eq. (2) (4.27 for ice XII vs 2.00 for ice VI; see Table III). For other ice structures, the coordination sequence has  $M_k$  values intermediate between those corresponding to ices VI and XII.

As indicated above, for a parabolic dependence of  $M_k$  as a function of the distance  $k$ , the ratio  $M_k/k^2$  should converge for large  $k$  to the coefficient  $a$ . For the ice structures considered here, this convergence is rather fast, as

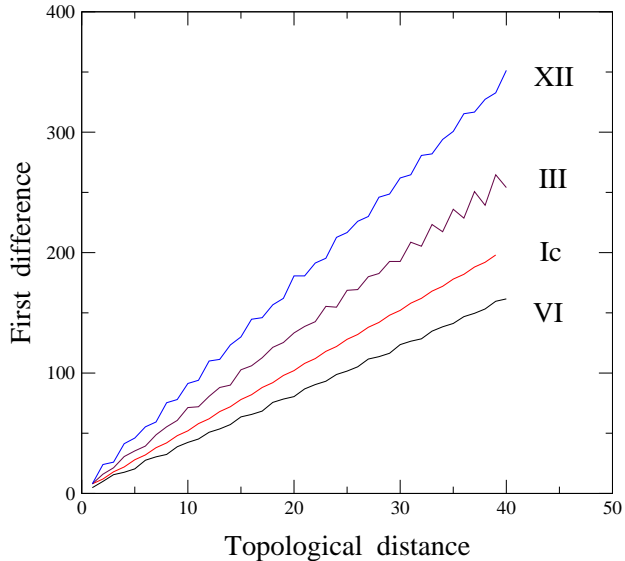


FIG. 3: First differences  $\delta_k$  of the coordination sequence  $\{M_k\}$  vs topological distance  $k$  for several ice structures. From top to bottom: ice XII, III, Ic, and VI.

shown in Fig. 2 for several cases. After some fluctuations for small  $k$ , for  $k \gtrsim 10$  that ratio converges rather smoothly to its high-distance limit. We observe again the clear differences between different ice structures. In particular, ices XII and VI have the largest and smallest  $a$  value, respectively. Note that the parabolic dependence of  $M_k$  is in general not strictly parabolic, although an equation such as Eq. (2) can fit very well the actual coordination sequences, with relative errors converging fast to zero as  $k$  increases.

To analyze with more detail the behavior of  $M_k$  vs  $k$  we consider the first and second differences,  $\delta_k$  and  $\epsilon_k$ , of the coordination sequences, defined in Eqs. (3) and (4), respectively. For a strict parabolic dependence of the form given in Eq. (2) one would expect a linear trend for the first differences:  $\delta_k = 2ak + a + b$ . The actual values of  $\delta_k$  for various ice structures are shown in Fig. 3. We observe for ice Ic that  $\delta_k$  follows closely a linear dependence on  $k$ , with small fluctuations around a straight line of slope  $2a$ . Such fluctuations are larger for ice VI, and they become more prominent for ices III and XII.

We now go to the second differences of the sequence  $\{M_k\}$ . For a strict parabolic dependence, one would have a constant value for the second differences:  $\epsilon_k = a$ . In Fig. 4 we display  $\epsilon_k$  as a function of  $k$  for ice Ih. The resulting  $\epsilon_k$  fluctuates between 2 and 3, in a periodic sequence with period length  $P = 4$ . Note that the mean value of this sequence is  $a = 2.625$ , which coincides with the value obtained from a direct fit for the sequence  $M_k$ . The characteristics of the sequence  $\{\epsilon_k\}$  depend strongly on the considered ice structure. Thus, in some cases one obtains a periodic sequence as in the case of ice Ih, and in other cases one finds a sequence  $\{\epsilon_k\}$  for which no

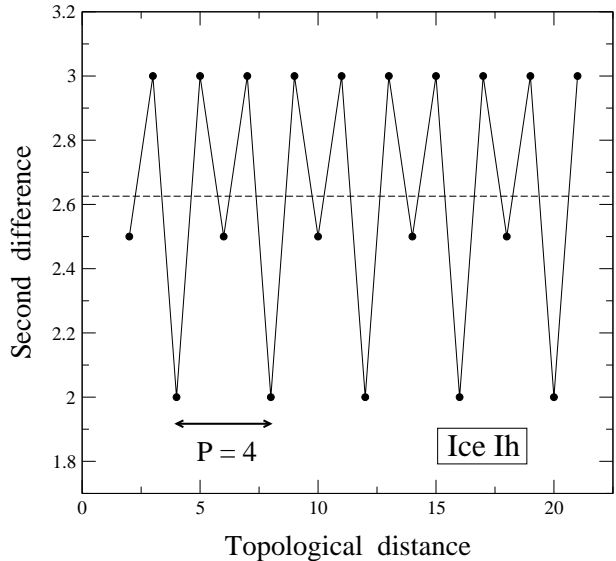


FIG. 4: Second differences  $\epsilon_k$  of the coordination sequence vs topological distance for ice Ih. The period length  $P = 4$  is indicated. The dashed line shows the parameter  $a$  corresponding to this structure.

regular pattern is easily found. The case of ice Ih is relatively simple in this respect, with a period  $P = 4$ . Even simpler is the structure of ice Ic, for which  $\{\epsilon_k\}$  alternates between two values (2 when  $k$  is even and 3 when it is odd), with an average  $a = 2.5$ . Note that this structure has the same topology as diamond, and is particularly simple to analyze. In fact, the exact value of  $M_k$  in this case is given by

$$M_k = \frac{5}{2}k^2 + \frac{3}{2}, \quad k = 2n + 1 \quad (11)$$

$$M_k = \frac{5}{2}k^2 + 2, \quad k = 2n + 2$$

for  $n = 0, 1, 2, \dots$

In other cases with a period length relatively small, it is not difficult to find exact expressions for  $M_k$ . For example, for ice II, with period length  $P = 4$ , one has (for  $k > 5$ ):

$$M_k = \frac{7}{2}k^2 - \frac{1}{2}k + c_k \quad (12)$$

where  $c_k = 2$  for  $k = 4n$  ( $n = 2, 3, 4, \dots$ ) and  $c_k = 1$  otherwise.

For other ice structures, we found sequences  $\{\epsilon_k\}$  with longer period lengths. The longest of them corresponds to ice XII, with  $P = 20$ . The sequence  $\{\epsilon_k\}$  for this ice structure is displayed in Fig. 5. One observes that a periodic sequence begins at  $k = 6$ , and two complete periods appear in the figure until  $k = 46$ . The mean value of  $\epsilon_k$  over a period is  $\bar{\epsilon}_k = 4.27$ , in agreement with the  $a$  value obtained from the parabolic fit of the sequence  $\{M_k\}$ , and shown in Table III.

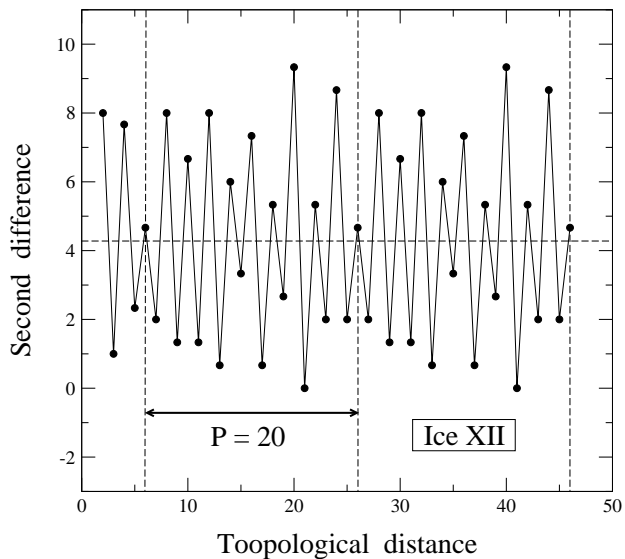


FIG. 5: Second differences  $\epsilon_k$  of the coordination sequence  $\{M_k\}$  vs topological distance for ice XII. The period length  $P = 20$  is displayed. The horizontal dashed line indicates the parameter  $a$  corresponding to this ice structure.

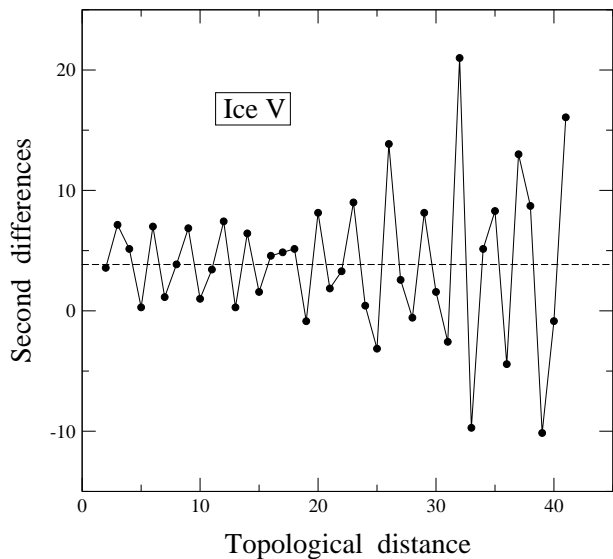


FIG. 6: Second differences  $\epsilon_k$  of the coordination sequence vs topological distance for ice V. The dashed line indicates the parameter  $a$  corresponding to this structure.

As mentioned above, there are other ice structures for which we could not find any repeated pattern in the sequence  $\{\epsilon_k\}$ . As an example, we display in Fig. 6  $\{\epsilon_k\}$  for ice V. We observe in this sequence that the values oscillate around the corresponding parameter  $a$  (horizontal dashed line), and the amplitude of the oscillations seems to increase as the distance  $k$  becomes larger. Among the ice structures considered here, we found three cases for which no periodic pattern appeared in the investigated  $k$ -region: ices III, IV, and V. This is indicated in the last column of Table III as ‘NP’. For the other structures (where a repeated pattern was found), a label ‘P’ indicates ‘periodic’, followed by a number referring to the period length. We note that two of the networks for which no periodic pattern in  $\{\epsilon_k\}$  has been found, are in some sense special, since ices III and V have been found to display partial hydrogen ordering. At present, we do not know any precise reason for this behavior and, although not probable, we cannot exclude an accidental coincidence. This point should be investigated in the near future.

Concerning the sequence  $\{\epsilon_k\}$ , we emphasize that in the cases where no periodicity was found, the existence of a period (maybe very long) cannot be excluded. In fact, really long periods have been found in some zeolite structures, using an algebraic description.<sup>21</sup> However, this is not crucial for our present purposes of comparing the topological density with other structural aspects of ice polymorphs.

### C. Topological density

The long-distance behavior of the coordination sequence  $\{M_k\}$  allows us to define the topological density of a given structure, as explained in Sect. II. The basic parameter for this purpose is the coefficient  $a$  of the quadratic term in Eq. (2). The topological density  $\rho$  takes values ranging from 2.5 (ice Ic) to 5 (ice VII) for the considered ice phases. In Table III we give for each structure the relative topological density  $\rho/\rho_{\text{Ih}}$  with respect to ice Ih. Note that hexagonal ice Ih and cubic ice Ic, although very similar in their local neighborhood have different topological density. Thus, for ice Ic  $\rho/\rho_{\text{Ih}} = 0.95$ , in agreement with the lower  $M_k$  values found for ice Ic, as compared to those of ice Ih.

In connection with our results for the topological density  $\rho$  of ice polymorphs, it is worthwhile mentioning that several authors have proposed to quantify the topological density in crystalline solids from the number of sites included in a cluster of a given topological radius,<sup>26</sup> using expressions such as  $S_k$  in Eq. (6). This definition, however, can lack an absolute meaning, as it yields values of the topological density which depend on the cluster size and on the normalization procedure. In this line, a more precise definition for the topological density of crystalline solids was given earlier as<sup>21,53</sup>

$$\rho' = \lim_{k \rightarrow \infty} \frac{S_k}{k^D} \quad (13)$$

( $D = 3$  here). As indicated above, for large  $k$  one has an asymptotic dependence for the mean coordination se-



quence:  $M_k \sim a k^2$  (see Eq. (1)), and therefore

$$S_k = \sum_{i=1}^k M_i \sim \frac{1}{3} a k^3 \quad (14)$$

as can be easily derived for the sum of squares of natural numbers. In this way one has  $\rho' = a/3$ . Note that this definition, apart from a factor 3 in the denominator, does not consider the number  $w$  of disjoint subnetworks in a given structure, as introduced in the present work.

Although one could in principle expect the existence of some relation between topological density and molar volume of the different ice structures, it is not evident that there is a close relation between both quantities. There are various reasons that can contribute to make difficult this comparison. The most important is the dependence of the molar volume on temperature and pressure in the parameter region where each phase is stable (or metastable), whereas the topological density is a fixed characteristic of each structure, irrespective of the value of external thermodynamic or mechanical variables. For this reason, we obtain a reference volume for each ice polymorph, representative of the corresponding phase and independent of external variables. Such a reference volume,  $v_0$ , can be considered as a fingerprint of the corresponding phase. To obtain  $v_0$ , we carry out a minimization procedure (at zero volume and temperature), in which atomic positions and cell parameters are optimized using the q-TIP4P/F interaction model, as described in Sect. II.

It can be argued that the use of an effective interatomic potential may introduce a bias in the reference volume of the different ice phases. This possible error, however, is not relevant for our present purposes, as differences in cell volumes derived from the q-TIP4P/F model and experimental data are smaller than 1%, in particular at low temperatures and relatively small external pressures.<sup>29,31</sup> A comparison of the volumes predicted by this and other interatomic potentials, including density-functional theory calculations, has been given elsewhere.<sup>54</sup> An advantage of the q-TIP4P/F model is that it allows us to optimize all degrees of freedom in relatively large unit cells with a reasonable computational effort.

In Fig. 7 we present the volume per molecule  $v_0$  vs the topological density  $\rho$  for crystalline ice structures. One observes that the data points are more or less aligned following a straight line of negative slope. However, the data corresponding to ices Ih, Ic, and XI depart from this line. This question will be discussed below.

It is important to recall that ice VII (along with ice VIII) and ice VI (along with ice XV) contain two independent subnetworks. This means that the total number of sites in each of these structures is twice that of a single subnetwork. Since the parameter  $a$  in these cases takes into account only sites in one subnetwork, for these structures the topological density  $\rho$  equals  $2a$  instead of  $a$  (see Sect. II). Data points corresponding to cases with two subnetworks ( $w = 2$ ) are displayed as open triangles in

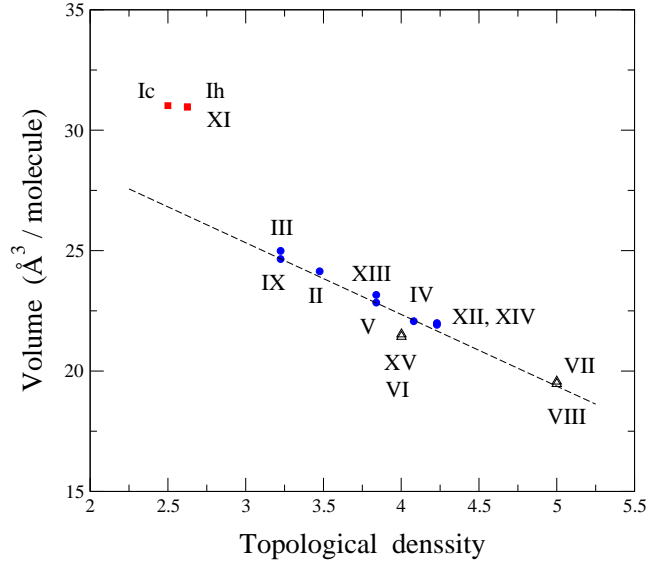


FIG. 7: Volume per molecule vs topological density  $\rho$  for several ice structures. Data points corresponding to networks with  $w = 2$  (ices VI, XV, VII, and VIII) are represented by open triangles.

Fig. 7. In connection with this, we remember that ice VII contains two subnetworks, each of them equivalent to the ice Ic network, so that the empty space has been filled by the two interpenetrating networks and the volume per molecule correlates well with the topological density, once the above-mentioned factor  $w = 2$  is included. In other words, for each subnetwork of ice VII, the parameter  $a$  coincides with that of ice Ic, but the topological density is twice larger in the former case than in the latter, so that ice VII appears in Fig. 7 following the trend of other ice polymorphs in the  $\rho-v_0$  plot. Something similar happens for ice VI.

According to the general trend observed in Fig. 7, one would expect for ices Ih and Ic (as well as ice XI) a volume per molecule smaller than that actually found. This has to be related to the rigidity of the H-bridges in these structures, along with the large empty space between water molecules, which makes that ices Ih and Ic have fairly open low-density structures, where the packing efficiency is low. Note that both ice structures contain only six-membered rings. The difference between them consists in the stacking sequence of layers formed by water molecules arranged in six-membered rings<sup>3,6,9</sup> ('chair' or 'boat' configurations). In practice, structural differentiation between ices Ic and Ih is complicated by the fact that ice Ic usually contains hexagonal stacking faults.<sup>55-57</sup>

The stiffness of ice Ic and Ih structures can be related to the rigidity of the tetrahedral arrangement of water molecules. In this line, several orientational parameters have been defined to measure the extent to which a molecule and its four nearest neighbors adopt a tetrahedral arrangement.<sup>58,59</sup> In particular, the order parameter  $q$  employed in Refs. 59,60 gives for the ideal crystal

structures of ice Ih and Ic its maximum value  $q = 1$ , which means that tetrahedra are undistorted. For other crystalline ice structures, this parameter is clearly lower than unity.

Another crystalline ice structure containing open channels is that of ice II, which presents one cavity per six water molecules.<sup>3</sup> The density of this ice polymorph is around 25% higher than that of ice Ih, but the former structure contains more roomy cavities than the latter.<sup>9</sup> We note that the similarity between channels in ices Ih and II is important for the mechanism of transition from one to the other.<sup>9</sup> However, concerning the rigidity of the tetrahedra in ice II, the situation is clearly different than ice Ih, as in the former case the tetrahedral order parameter takes a value  $q = 0.83$ , clearly lower than in the case of ice Ih. This indicates an appreciable distortion of the tetrahedra of water molecules in the case of ice II.

In connection with the topological characterization of ice polymorphs, an interesting question is its generalization to other phases, such as amorphous ice and confined water. For amorphous ice, in particular, a topological density  $\rho$ , similar to that discussed here for crystalline phases, could be defined. Given the three-dimensional character of the amorphous H-bond networks, one expects to find average coordination sequences  $\{M_k\}$  with a distance dependence similar to Eq. (1). This can allow to study the correlation between topological density and actual molar volume of the amorphous phases.

#### IV. CONCLUDING REMARKS

We have presented an analysis of the ring statistics and coordination sequences in crystalline ice structures. This

has allowed us to quantitatively characterize the topology of different ice polymorphs. In particular, an analysis of the coordination sequences up to large distances provides us with a quantitative measure of the topological density of the corresponding networks. This measure is obtained from the coefficient  $a$  derived from the parabolic dependence of the coordination sequence on the topological distance.

We have found a correlation between the topological density  $\rho$  and crystal volume of the considered ice polymorphs. The general trend shown in Fig. 7 is apparently not followed by ices Ih and Ic, due to the low density and rigidity of these structures.

Other ways of characterizing the different ice networks can give further insight into the structural properties of different polymorphs. In this line, we mention the use of the so-called connective constants, derived from self-avoiding walks in networks, to study complex crystal structures such as those of zeolites.<sup>61</sup> All this can help to understand thermodynamic properties of solid water phases, as the configurational entropy associated to hydrogen disorder, which is known to depend on the topology of ice networks.<sup>62,63</sup>

#### Acknowledgments

This work was supported by Dirección General de Investigación (Spain) through Grant FIS2012-31713, and by Comunidad Autónoma de Madrid through Program MODELICO-CM/S2009ESP-1691.

- 
- <sup>1</sup> A. N. Dunaeva, D. V. Antsyshkin, and O. L. Kuskov, *Solar System Research* **44**, 202 (2010).
- <sup>2</sup> T. Bartels-Rausch, V. Bergeron, J. H. E. Cartwright, R. Escribano, J. L. Finney, H. Grothe, P. J. Gutierrez, J. Haapala, W. F. Kuhs, J. B. C. Pettersson, et al., *Rev. Mod. Phys.* **84**, 885 (2012).
- <sup>3</sup> C. G. Salzmann, P. G. Radaelli, B. Slater, and J. L. Finney, *Phys. Chem. Chem. Phys.* **13**, 18468 (2011).
- <sup>4</sup> E. A. Zheligovskaya and G. G. Malenkov, *Russian Chem. Rev.* **75**, 57 (2006).
- <sup>5</sup> D. Eisenberg and W. Kauzmann, *The Structure and Properties of Water* (Oxford University Press, New York, 1969).
- <sup>6</sup> V. F. Petrenko and R. W. Whitworth, *Physics of Ice* (Oxford University Press, New York, 1999).
- <sup>7</sup> G. W. Robinson, S. B. Zhu, S. Singh, and M. W. Evans, *Water in Biology, Chemistry and Physics* (World Scientific, Singapore, 1996).
- <sup>8</sup> J. D. Bernal and R. H. Fowler, *J. Chem. Phys.* **1**, 515 (1933).
- <sup>9</sup> G. Malenkov, *J. Phys.: Condens. Matter* **21**, 283101 (2009).
- <sup>10</sup> W. B. Pearson, *The crystal chemistry and physics of metals and alloys* (Wiley, New York, 1972).
- <sup>11</sup> A. F. Wells, *Structural inorganic chemistry* (Clarendon Press, Oxford, 1986), 5th ed.
- <sup>12</sup> F. Liebau, *Structural chemistry of silicates: structure, bonding, and classification* (Springer, Berlin, 1985).
- <sup>13</sup> V. A. Blatov, *Acta Cryst. A* **56**, 178 (2000).
- <sup>14</sup> I. A. Baburin and V. A. Blatov, *Acta Cryst. B* **63**, 791 (2007).
- <sup>15</sup> S. J. Singer and C. Knight, *Adv. Chem. Phys.* **147**, 1 (2012).
- <sup>16</sup> C. Knight, S. J. Singer, J. L. Kuo, T. K. Hirsch, L. Ojamae, and M. L. Klein, *Phys. Rev. E* **75**, 056113 (2006).
- <sup>17</sup> C. Knight and S. J. Singer, *J. Chem. Phys.* **129**, 164513 (2008).
- <sup>18</sup> W. M. Meier and H. J. Moeck, *J. Solid State Chem.* **27**, 349 (1979).
- <sup>19</sup> G. O. Brunner, *J. Solid State Chem.* **29**, 41 (1979).
- <sup>20</sup> J. H. Conway and N. J. A. Sloane, *Proc. R. Soc. London A* **453**, 2369 (1997).
- <sup>21</sup> R. W. Grosse-Kunstleve, G. O. Brunner, and N. J. A. Sloane, *Acta Cryst. A* **52**, 879 (1996).

- <sup>22</sup> L. Stixrude and M. S. T. Bukowinski, *Am. Miner.* **75**, 1159 (1990).
- <sup>23</sup> C. P. Herrero, *J. Chem. Soc.: Faraday Trans.* **90**, 2597 (1994).
- <sup>24</sup> J. G. Eon, *Acta Cryst. A* **58**, 47 (2002).
- <sup>25</sup> C. P. Herrero, *Phys. Rev. E* **66**, 046126 (2002).
- <sup>26</sup> G. O. Brunner, *Zeolites* **13**, 88 (1993).
- <sup>27</sup> S. Habershon, T. E. Markland, and D. E. Manolopoulos, *J. Chem. Phys.* **131**, 024501 (2009).
- <sup>28</sup> R. Ramírez and C. P. Herrero, *J. Chem. Phys.* **133**, 144511 (2010).
- <sup>29</sup> C. P. Herrero and R. Ramírez, *J. Chem. Phys.* **134**, 094510 (2011).
- <sup>30</sup> B. S. Gonzalez, E. G. Noya, C. Vega, and L. M. Sese, *J. Phys. Chem. B* **114**, 2484 (2010).
- <sup>31</sup> R. Ramírez, N. Neuerburg, M. V. Fernández-Serra, and C. P. Herrero, *J. Chem. Phys.* **137**, 044502 (2012).
- <sup>32</sup> W. H. Zachariasen, *J. Am. Chem. Soc.* **54**, 3841 (1932).
- <sup>33</sup> J. D. Bernal, *Proc. Roy. Soc. London A* **280**, 299 (1964).
- <sup>34</sup> S. V. King, *Nature* **213**, 1112 (1967).
- <sup>35</sup> L. Stixrude and M. S. T. Bukowinski, *Science* **250**, 541 (1990).
- <sup>36</sup> L. Guttman, *J. Non-Cryst. Solids* **116**, 145 (1990).
- <sup>37</sup> C. S. Mariani and L. W. Hobbs, *J. Non-Cryst. Solids* **124**, 242 (1990).
- <sup>38</sup> K. Goetzke and H. J. Klein, *J. Non-Cryst. Solids* **127**, 215 (1991).
- <sup>39</sup> X. L. Yuan and A. N. Cormack, *Comp. Mater. Sci.* **24**, 343 (2002).
- <sup>40</sup> J. S. Loveday and R. J. Nelmes, *Phys. Chem. Chem. Phys.* **10**, 937 (2008).
- <sup>41</sup> M. Weinwurm and C. Dellago, *J. Phys. Chem. B* **115**, 5268 (2011).
- <sup>42</sup> G. Zhang, W. Zhang, and H. Dong, *J. Chem. Phys.* **133**, 134703 (2010).
- <sup>43</sup> O. Byl, J.-C. Liu, Y. Wang, W.-L. Yim, J. K. Johnson, and J. T. Yates, Jr., *J. Am. Chem. Soc.* **128**, 12090 (2006).
- <sup>44</sup> S. Ghosh, K. Ramanathan, and A. Sood, *Europhys. Lett.* **65**, 678 (2004).
- <sup>45</sup> A. I. Kolesnikov, J. M. Zanotti, C. K. Loong, P. Thiyagarajan, A. P. Moravsky, R. O. Loutfy, and C. J. Burnham, *Phys. Rev. Lett.* **93**, 035503 (2004).
- <sup>46</sup> Y. Maniwa, H. Kataura, M. Abe, A. Udaka, S. Suzuki, Y. Achiba, H. Kira, K. Matsuda, H. Kadowaki, and Y. Okabe, *Chem. Phys. Lett.* **401**, 534 (2005).
- <sup>47</sup> J. S. Tse, D. D. Klug, M. Guthrie, C. A. Tulk, C. J. Benmore, and J. Urquidi, *Phys. Rev. B* **71**, 214107 (2005).
- <sup>48</sup> C. G. Salzmann, T. Loerting, S. Klotz, P. W. Mirwald, A. Hallbrucker, and E. Mayer, *Phys. Chem. Chem. Phys.* **8**, 386 (2006).
- <sup>49</sup> J. L. Finney, A. Hallbrucker, I. Kohl, A. K. Soper, and D. T. Bowron, *Phys. Rev. Lett.* **88**, 225503 (2002).
- <sup>50</sup> C. A. Tulk, C. J. Benmore, J. Urquidi, D. D. Klug, J. Neufeind, B. Tomberli, and P. A. Egelstaff, *Science* **297**, 1320 (2002).
- <sup>51</sup> D. T. Bowron, J. L. Finney, A. Hallbrucker, I. Kohl, T. Loerting, E. Mayer, and A. K. Soper, *J. Chem. Phys.* **125**, 194502 (2006).
- <sup>52</sup> J. M. Ziman, *Models of disorder* (Cambridge University, Cambridge, 1979).
- <sup>53</sup> J. G. Eon, *Acta Cryst. A* **60**, 7 (2004).
- <sup>54</sup> B. Pamuk, J. M. Soler, R. Ramírez, C. P. Herrero, P. W. Stephens, P. B. Allen, and M. V. Fernández-Serra, *Phys. Rev. Lett.* **108**, 193003 (2012).
- <sup>55</sup> G. P. Arnold, E. D. Finch, S. W. Rabideau, and R. G. Wenzel, *J. Chem. Phys.* **49**, 4365 (1968).
- <sup>56</sup> I. Kohl, E. Mayer, and A. Hallbrucker, *J. Phys. Chem. B* **104**, 12102 (2000).
- <sup>57</sup> C. G. Salzmann, E. Mayer, and A. Hallbrucker, *Phys. Chem. Chem. Phys.* **6**, 1269 (2004).
- <sup>58</sup> P. L. Chau and A. J. Hardwick, *Mol. Phys.* **93**, 511 (1998).
- <sup>59</sup> J. R. Errington and P. G. Debenedetti, *Nature* **409**, 318 (2001).
- <sup>60</sup> C. McBride, E. G. Noya, J. L. Aragones, M. M. Conde, and C. Vega, *Phys. Chem. Chem. Phys.* **14**, 10140 (2012).
- <sup>61</sup> C. P. Herrero, *J. Phys.: Condens. Matter* **7**, 8897 (1995).
- <sup>62</sup> C. P. Herrero and R. Ramírez, *Chem. Phys. Lett.* **568-569**, 70 (2013).
- <sup>63</sup> L. G. MacDowell, E. Sanz, C. Vega, and J. L. F. Abascal, *J. Chem. Phys.* **121**, 10145 (2004).
- <sup>64</sup> S. W. Peterson and H. A. Levy, *Acta Cryst.* **10**, 70 (1957).
- <sup>65</sup> H. König, *Z. Kristallogr.* **105**, 279 (1944).
- <sup>66</sup> B. Kamb, W. C. Hamilton, S. J. LaPlaca, and A. Prakash, *J. Chem. Phys.* **55**, 1934 (1971).
- <sup>67</sup> C. Lobban, J. L. Finney, and W. F. Kuhs, *J. Chem. Phys.* **112**, 7169 (2000).
- <sup>68</sup> H. Engelhardt and B. Kamb, *J. Chem. Phys.* **75**, 5887 (1981).
- <sup>69</sup> W. F. Kuhs, J. L. Finney, C. Vettier, and D. V. Bliss, *J. Chem. Phys.* **81**, 3612 (1984).
- <sup>70</sup> C. Lobban, J. L. Finney, and W. F. Kuhs, *Nature* **391**, 268 (1998).